IEEE Access
Multidisciplinary ⋮ Rapid Review ⋮ Open Access Journal

Received 6 May 2024, accepted 28 May 2024, date of publication 3 June 2024, date of current version 10 June 2024.

Digital Object Identifier 10.1109/ACCESS.2024.3408239

RESEARCH ARTICLE

Techno-Economic and Sensitivity Analysis of Grid Connected Perovskite PV-Wind Systems

MASOOD IBNI NAZIR[1], (Member, IEEE), F. SELIM[2], AIJAZ AHMAD[3], (Member, IEEE), IKHLAQ HUSSAIN[3], SAMIR M. DAWOUD[1,4], KHALIL ALLUHAYBI[5], (Member, IEEE), AND ALAA A. ZAKY[1,2]

[1]Department of Electrical Engineering, College of Engineering and Information Technology, Onaizah Colleges, Qassim 56447, Saudi Arabia
[2]Electrical Engineering Department, Faculty of Engineering, Kafrelsheikh University, Kafr El Sheikh 33511, Egypt
[3]Department of Electrical Engineering, National Institute of Technology, Srinagar 190006, India
[4]Department of Electrical Power and Machines Engineering, Faculty of Engineering, Tanta University, Tanta 31512, Egypt
[5]Department of Electrical Engineering, College of Engineering, Taibah University, Al-Madinah al-Munawwarah 42353, Saudi Arabia

Corresponding author: Masood Ibni Nazir (masoodnazir111@gmail.com)

ABSTRACT This work proposes the techno-economic analysis of a three-phase, three wire grid integrated third-generation perovskite solar cells-wind energy conversion system (PSC-WECS) controlled by a two-level voltage source converter (VSC) which is driven by the application of polynomial zero-attracting least mean square (PZA-LMS) algorithm. The proposed algorithm enhances the dynamic performance of the system by introducing sinusoidal grid currents with low total harmonic distortion (THD) which enhances system performance by providing acceptable outcomes under dynamic loading, fluctuating wind velocity, and solar insolation by compensating for load reactive power and balancing load and power demands at the point of coupling. This work replaces the conventional silicon PVs with PSCs to improve the economics of power generation thanks to their higher efficiency. For relative comparisons, the performance of the proposed 36 kW PSC-WECS is compared with the conventional silicon PV-WECS. The results reveal that the proposed system has a low net present cost (NPC) of $68843 compared to the conventional system which costs $160917, translating to a reduction of 58% in total cost. Sensitivity Analysis (SA) is performed to analyse the dependence of optimal solutions on the uncertainty of key variables namely NPC, cost of energy (COE), windspeed & insolation. The results show that the total NPC is more sensitive to the COE and the average wind speed as compared to the other variables. Moreover, the area covered by the proposed system is reduced by 50% while as the cost of power generation is reduced by 72% due to the high efficiency of PSCs. The results obtained in MATLAB/Simulink and HOMER to determine the optimum quantity of the renewable energy sources (RES) model demonstrate the effectiveness of the recommended system.

INDEX TERMS Perovskite PV systems, sensitivity analysis, techno-economics, wind energy systems.

NOMENCLATURE

SA	Sensitivity Analysis.
PV	Photo-Voltaic.
UV	Ultra-Violet.
BC	Boost Converter.
WT	Wind Turbine.
RF	Renewable Fraction.
VSC	Voltage Source Converter.
THD	Total Harmonic Distortion.
P&O	Perturb & Observe.
NPC	Net Present Cost.
COE	Cost of Energy.
RES	Renewable Energy Sources.
SSC	Silicon Solar Cells.
PSC	Perovskite Solar Cell.
VOC	Open Circuit Voltage.
MPP	Maximum Power Point.
NLL	Non Linear Load.
LMS	Least Mean Square.
LMF	Least Mean Fourth.
ANN	Artificial Neural Network.

The associate editor coordinating the review of this manuscript and approving it for publication was Inam Nutkani.

ARV	Adaptive Reference Voltage.
PCC	Point of Common Coupling.
CRF	Capital Recovery Factor.
O&M	Operation & Maintenance.
WECS	Wind Energy Conversion Systems.
MPPT	Maximum Power Point Tracking.
LLAD	Leaking Logarithmic Absolute Difference.
LMMN	Least Mean Mixed Norm.
ZALMS	Zero Attracting Least Mean Square.
LLMLF	Least Leaking Mean Logarithmic Fourth.
LLMLF	Leat Leaking Mean Logarithmic Fourthe.
RLMLS	Robust Least Mean Logarithmic Square.
FXLMF	Filtered-X Least Mean Fourth.
PZALMS	Polynomial Zero Attracting Least Mean Square.
PSC-WECS	Perovskite Solar Cell Wind Energy Conversion Systems.

I. INTRODUCTION

Renewable energy systems (RES) have emerged as a crucial component of the global shift towards sustainable and environmentally friendly energy sources. They offer a sustainable and clean alternative for meeting the world's energy needs and encompass a diverse range of technologies especially photovoltaic (PV) systems and wind energy conversion systems (WECS) that harness solar and wind energy to generate power. Among the various technologies used to harness solar energy, silicon solar cells (SSCs) have been widely adopted. Although they have been used extensively over the years and offer several advantages which include high reliability, easy scalability and long-term performance, they come with certain drawbacks that may have hindered their widespread implementation. The manufacturing process of SSCs involves high production costs, primarily due to the energy-intensive production of pure silicon and the complex manufacturing techniques required. Their efficiency is limited especially under low-light conditions which limits their overall energy output. They are relatively fragile and can be prone to damage from external factors like temperature variations and moisture which increases the maintenance and replacement costs. To address these drawbacks, sustained research efforts are focussed to develop alternatives with improved efficiency, decreased capital costs and improved environmental sustainability. These include thin-film solar cells and perovskite solar cells (PSCs) which offer higher efficiency, lower production costs, and improved environmental performance.

The third-generation PSCs are extremely affordable, highly efficient solar cells that are manufactured by incorporating structural changes at the nanotechnology level [1] with an acclaimed power conversion efficiency of 25% [2]. This efficiency can be increased even further by making use of surface passivation of the electron transporting and perovskite layers [3]. Doping improves the photovoltaic performance of the PSCs [3] in addition to ameliorating thermal and ambient stabilities. By enhancing their open circuit voltage (VOC), all-inorganic and tin-based perovskites have the potential to exceed the Shockley– Queisser (S–Q) limitations. Moreover, PSCs are environment friendly as their constituents comprising bismuth, cesium and formamidinium iodides are relatively less toxic as compared to methylammonium iodide of silicon technology. This indicates that perovskite cells will fully phase out silicon-based cells in the near future. The detailed fabrication, modelling and characterisation of PSC PV systems is detailed in [4], [5], and [6]. Nevertheless, ultraviolet (UV) light, oxygen, and moisture can all contribute to the poor stability of polycrystalline perovskite materials which needs immediate addressal. The state-of-the-art perovskite semi-transparent top cells have exhibited negligible degradation (<4%) after 1000 hours of continuous operation at MPP near 60°C [7]. This has proved to be a shot in the arm for PSC technology and it depicts its stability under adverse conditions. The state of the art in techno-economic and sensitivity analysis of grid-connected systems involves a comprehensive examination of various factors influencing the viability, performance, and economics of such systems. The techno-economic analysis includes information about system components, system design, levelized cost of electricity, and lifetime analysis [8], [9]. On the other hand, sensitivity analysis includes parameter variation, scenario analysis and uncertainty management [10].

The integration of RES with the grid is challenging owing to the intermittency of solar and wind energy which leads to challenges in stabilising grid frequency and voltage in addition to creating voltage problems on the load side, reverse power flow, harmonics, voltage sag and swell. Such problems are addressed by employing efficient control algorithms to approximate the component of reference current resulting in the generation of appropriate gating pulses for the voltage source converters (VSCs) which helps to reduce grid pressure by optimizing the resource utilization factor under varying environmental conditions. Numerous adaptive controls have been applied in the fields of pattern identification and signal processing. The adaptive controls like least mean square (LMS) [11] and least mean fourth (LMF) [12] have reduced computational difficulty with high steady-state error. Advanced algorithms like the leaky least mean logarithmic fourth (LLMLF) [13], zero-attracting least mean square (ZALMS) [14], robust least mean logarithmic square (RLMLS) [15], leaky least logarithmic absolute difference (LLLAD) [16], filtered – X least mean fourth (FXLMF) [17] and least mean mixed norm (LMMN) [18] algorithms produce reduced error and exhibit greater noise repudiation capability. LLMLF can be tuned comfortably, exhibits swift confluence, and produces minimum steady state error [13]. System identification is challenging in RZA-LMS which is complex and uses a starting variable to create a fluctuating step size [14]. The leaky idea enhances the learning process of LLLAD control which converges rapidly by using the logarithm of absolute deviation of error [16].

Wind and PV driven RES must deal with the environmental intermittency by consistently tracking the maximum power

point (MPP) and generate optimum system power. Many maximum power point tracking (MPPT) techniques in grid connected RES have been reported which include the fuzzy logic control, perturb and observe method (P&O), and evolutionary algorithms. The P&O algorithm is commonly reported due to its ease of application as it involves perturbing the system in the direction of peak power. A comprehensive review of various MPPT techniques in a grid-connected RES in terms of convergence speed and initial parameters is mentioned in [19]. A thorough evaluation of performance validating the potency of the MPPT technique of a grid connected RES is presented in [20]. A search space minimization-based PSO algorithm to track MPPT under abrupt windspeed variations in a WECS is proposed in [21].

This study proposes an optimal hybrid power system considering the technical, economic, and environmental factors of setting up a grid connected perovskite PV-wind hybrid system by comparing the cost & efficiency of a perovskite PV system with the conventional silicon PV system. The proposed model provides the same amount of power as is provided by the conventional hybrid system albeit at a much lower cost and area. In previous studies, the manufacturing costs for PSCs have been reported to be between (20)–40) $\$/m^2$ which is significantly lower than those reported for silicon PV cells (50–80) $\$/m^2$. This decreases the cost of generation of electricity in PSCs from (0.24-0.46) \$/W in silicon solar cells to 0.16 \$/W in PSCs [22], [23].

HOMER ranks simulation outcomes based on net present cost (NPC) with the lowest value representing the best configuration. This study also performs SA [24], [25], [26] of the hybrid system to reflect on the effect of varying insolation & windspeed on this system. The technical prowess of this PSC-WECS is tested by integrating this system with a three-phase grid that feeds power to NLLs besides possessing capacity to recompense loads under changing wind velocity, irradiation, and NLL unbalancing. The polynomial zero attracting LMS (PZALMS) control [27], [28] extracts precise fundamental load current component, I_{loss}, to generate accurate gating pulses for the VSC to regulate the DC link voltage (V_{dc}) besides performing other functions viz; reactive power assistance, augmentation in power factor and load balancing. The proposed results depict the efficiency of the perovskite PV-wind hybrid system over the conventional hybrid system.

The main objectives of the proposed work are:

1) To analyse several components and design outputs, find cost-competitive points for perovskite PV – wind systems, and identify the best cost-effective design.
2) To verify the efficacy of the proposed control and the resulting system robustness by performing SA under varied irradiance and wind-speeds to evaluate the return on investment of the proposed optimised hybrid system.
3) Maximizing annual utility bill savings & improved efficiency.

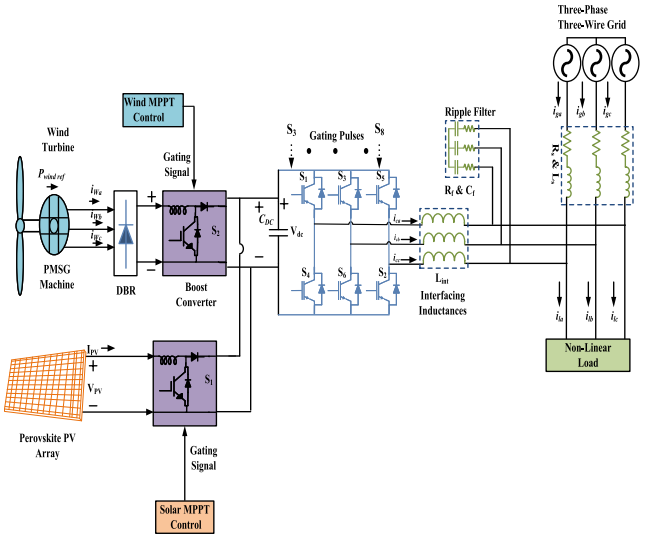

FIGURE 1. System topology.

4) Regulating V_{dc}: The PZALMS control regulates V_{dc} by generating accurate I_{loss} and weight signal components to enhance VSC performance during unbalanced loading and under varying wind-speeds and irradiation.

The proposed system is simulated in MATLAB/Simulink & HOMER.

II. SYSTEM DESCRIPTION AND PARAMETER SELECTION

The topology of the three-phase grid connected PSC - WECS system is illustrated in Fig. 1. It comprises a 32.5 kW perovskite PV system and a 3.5 kW WECS which is linked with a 700 V DC bus. The interfacing inductances reduce the ripple content while as the RC filter accounts for the harmonic suppressions. A varying NLL of 7 kW is connected at the load side. The detailed modelling of this system is mentioned in [14]. The design of the boost converter, the DC link capacitor, the interfacing inductor and the RC filter is detailed in the subsequent section.

1) DESIGN OF BOOST CONVERTER

The capacitance, inductance and the duty cycle (D) of the boost converter (BC) are calculated as [29]:

$$V_{out} = \frac{V_{in}}{1-D} \tag{1}$$

$$L = V_{in}\frac{V_{out}-V_{in}}{i_{ripple}}f_s V_{out} \tag{2}$$

$$C = I_{out}\frac{D}{\delta V f_s} \tag{3}$$

where, f_s denotes the switching frequency and is equal to 20 kHz, V_{in} is the voltage present at the input side of BC, V_{out} is the output voltage of DC bus and δV is the permissible contortion band of voltage which is equivalent to 1-2% of V_{out}. An inductance of L = 4.5 mH is used here.

TABLE 1. Characteristic comparison between SSC, PSC and the Bergey wind turbine.

Parameters	Silicon solar cells	Perovskite solar cells	WT Bergey Excel 10-R
Power rate	32.5 kW	32.5 kW	3.5 kW
Derating factors	85%	85%	-
Capital cost	$700/kW	$200/kW	$13250/Unit
Replacement cost	$1400	$180	$13250/Unit
Operating and main taining cost	Negligible	Negligible	$132.5
Lifespan	25	25	20

2) DESIGN OF FILTER AND INTERFACING INDUCTOR

The RC filter sieves out noise from voltage at PCC. The ripple filter details used in this work are $R_f = 5\Omega$ and $C_f = 5\mu$F and $R_f C_f = Ts/10$.

where R_f, C_f = RC filter resistor and capacitor, T_s = switching time [29]. The calculated value of the interfacing inductance used here is 5.2 mH.

3) DESIGN OF DC LINK CAPACITANCE

The DC link capacitance is calculated as [29]

$$\frac{1}{2}C_{DC}(V_{DC}^2 - V_{DCmin}^2) = k3VqIt \tag{4}$$

where V_{DC} = Reference DC voltage, V_{DCmin} = Minimum DC voltage, q = burdening factor = 1, V, I = phase voltage, current and t is the time by which the DC bus voltage is to be recovered. In this work, $C_{DC} = 10000\mu$F.

The least magnitude of DC bus voltage is greater than two times the peak of phase voltage. It is given as

$$V_{DC} = \frac{2\sqrt{2}V_{LL}}{\sqrt{3}p} \tag{5}$$

where p is the modulation index = 1 and V_{LL} = line to line output voltage. V_{DC} thus calculated is 677.7V≈ 700V.

4) DESIGN OF PSC & HOMER SYSTEM INPUTS

The grid-connected RES has four important components namely the grid, the wind turbine (WT), the VSC, and the PSC array. HOMER is used to determine the optimal size for the different system components considering their capacity to ensure preciseness and accuracy. The economic and technical parameters of the PV, WT and the converter system is depicted in Table 1. The PSC parameters like open circuit voltage, short circuit current, external and internal quantum efficiency are computed using a solar simulator. The fabricated PSC has a short circuit current density of 23.5 mA/cm^2, open circuit voltage of 1.085 V, and fill factor of 0.79. The power rate of the converter is 40 kW, capital cost is $500/kW, renewal cost is $450/kW, operating and maintenance (O&M) cost is $50/year, lifespan is 15 years and efficiency is 90%. The project life time for this system is 25 years at an interest rate of 8% annually with zero capacity shortage. All these values are input in HOMER pro to evaluate constraints regarding the required load, rating of PV - wind system and different components involved in this work. After analysis, this data is fed to the software to obtain optimized results along with the results of SA based on NPC and cost of energy (COE). All the data regarding PSC PV, WECS and HOMMER inputs are detailed in Table 1.

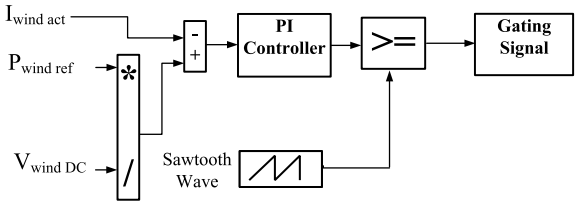

FIGURE 2. Wind MPPT control.

III. ECONOMIC AND ENVIRONMENTAL PARAMETERS

The NPC and the renewable fraction (RF) are the chief variables needed to determine the optimal solution. The NPC [30] includes all the earnings and costs incurred during the course of a project. It is calculated from Eq. (6).

$$NPC = \frac{C_{att}}{CRF(i, T_p)} \tag{6}$$

where C_{att}, i and T_p denote the annual cost, the annual real interest rate (%), and the lifetime of the project, respectively. The capital recovery factor (CRF) term is evaluated using Eq. (7):

$$CRF = \frac{d(1+d)^T}{d(1+d)-1} \tag{7}$$

where T depicts the year number, and d is the appropriate discount rate.

RF denotes the fraction of power consumed by the load from the RES. It is given by Eq. (8).

$$RF = 1 - \frac{E_{nonren} + H_{nonren}}{E_{served} + H_{served}} \tag{8}$$

where E_{nonren} is the non-renewable electrical production, H_{nonren} is the non-renewable thermal production, E_{served} is the total electrical load served, and H_{served} is the total thermal load served. All these quantities are expressed in kWh/year.

COE is calculated by taking the ratio of the yearly cost of electricity production to the total load served and is given by Eqs. (9) & (10).

$$COE = \frac{C_{an,total}}{E_{served}} \tag{9}$$

$$COE = \frac{C_{an,total}}{AC_{load} + DC_{load}} \tag{10}$$

IV. VSC CONTROL

The suggested setup is run such that the point in tune with the MPP is pursued consistently by monitoring the circuit DC current. The arrangement comprises solar & wind MPPT control & the converter control which is discussed in the following section.

A. WIND MPPT SCHEME

The WECS utilizes a proportional integral (PI) controller (Fig. 2) to generate optimal output by minimising the error involving the requisite & the true current to zero [18]. The input signal is given by Eq. (11).

$$I_{wind,err} = \frac{P_{wind,ref}}{V_{windDC}} \tag{11}$$

where P_{wind} and v_{wind} depict the output power and voltage of the WECS.

B. PV MPPT SCHEME

P&O technique is used to extract optimum output to control the BC's output by monitoring its input voltage and current while ensuring a suitable duty cycle. The rated capacity of the PV array used here is 32.5 kW.

C. PZALMS CONTROL

This paper proposes a polynomial zero attracting LMS (PZALMS) control [27], [28] (Fig. 3) for the generation of VSC gating pulses. The objective function of PZA-LMS comprises the combination of l_0 and l_2 norms for system identification purposes. The l_0 norm is calculated from an α order polynomial to help speed up convergence and improve filtering. This control generates accurate weight signals and I_{loss} helping the VSC to perform multifunctional operations like PQ improvement, supplying required load reactive power, and balancing active power.

The update rule governing the weight equations is given as

$$W_i(n+1) = W_i(n) - \mu \frac{\partial \zeta_{l2}(n)}{\partial W_i(n)} - \mu\gamma \frac{\partial \zeta_{l0}(n)}{\partial W_i(n)} \tag{12}$$

The 2nd & 3rd terms in this equation are calculated from Eqs. (13) & (14).

$$\frac{\partial \zeta_{l2}(n)}{\partial W_i(n)} = -e_n \mu_{p\gamma} \tag{13}$$

$$\frac{\partial \zeta_{l0}(n)}{\partial W_i(n)} = g_{p\gamma} = \begin{cases} \dfrac{sgn[W_i(k)][1-(\alpha-1)|W_i(k)|]}{[1+|W_i(k)|]^{\alpha+1}}; \\ |W_i(k)| \leq \dfrac{1}{\alpha-1} \\ 0; \textit{Otherwise} \end{cases} \tag{14}$$

where α denotes the polynomial term that has an inverse variation with the zero-attracting term.

The unit templates are computed as [14]:

$$\mu_{pa} = \frac{v_{sa}}{v_t}; \mu_{pb} = \frac{v_{sb}}{v_t}; \mu_{pc} = \frac{v_{sc}}{v_t} \tag{15}$$

where μ_{pa}, μ_{pb}, and μ_{pc} represent the unit templates in a, b and c phases, respectively. v_t is the voltage at PCC and is given by

$$V_t = \sqrt{2/3(v_{sa}^2 + v_{sb}^2 + v_{sc}^2)} \tag{16}$$

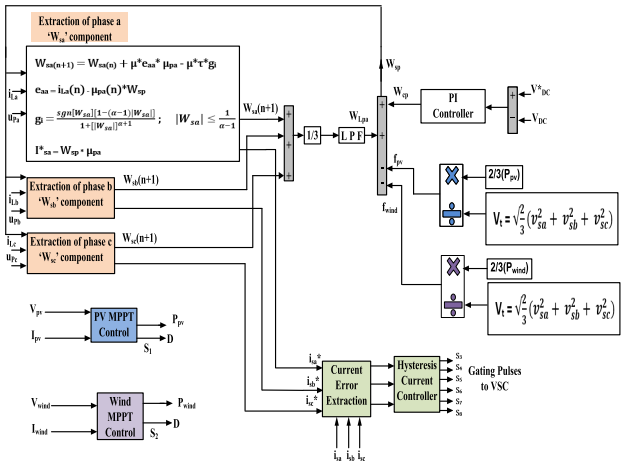

FIGURE 3. PZALMS Control.

where v_{sa}, v_{sb} and v_{sc} are the phase voltages of a, b and c phases, respectively. The corresponding error is computed from the unit templates and is given by Eq. (17).

$$e_{p_\gamma} = i_{L_\gamma} - \mu_{p_\gamma} W_{sp} \tag{17}$$

where $\gamma = a, b, c$ for a, b & c phase, respectively. $i_{L\gamma}$ is the load current and W_{sp} is the total weight of the fundamental active component.

The corresponding active weight components for the three phases are calculated from Eqs. (18), (19) & (20).

$$W_{sa}(n+1) = W_{sa}(n) + \mu\mu_{pa}e_{pa}(n) - \mu\tau g_{pa}(n) \tag{18}$$

$$W_{sb}(n+1) = W_{sb}(n) + \mu\mu_{pb}e_{pb}(n) - \mu\tau g_{pb}(n) \tag{19}$$

$$W_{sc}(n+1) = W_{sc}(n) + \mu\mu_{pc}e_{pc}(n) - \mu\tau g_{pc}(n) \tag{20}$$

The terms g_{pa}, g_{pb} & g_{pc} are computed from Eq. 14 while as Eq. 17 is used to compute the terms e_{pa}, e_{pb} & e_{pc}.

The norm of the fundamental active component is computed by adding Eqs. (18), (19) & (20) and is given by Eq. (21).

$$W_p = \frac{1}{3}(W_{sa} + W_{sb} + W_{sc}) \tag{21}$$

f_{wind} is used to encompass wind changes and is given as

$$f_{wind} = \frac{2P_{wind}}{3V_t} \tag{22}$$

The reference supply currents are given by Eq. (23).

$$i_{sa}^* = W_{sp} * \mu_{pa};\ i_{sb}^* = W_{sp} * \mu_{pb};\ i_{sc}^* = W_{sp} * \mu_{pc} \tag{23}$$

V. RESULTS

The proposed system comprises a PSC PV-WECS that is integrated with the grid at 415 V, 50 Hz. The PSC PV & wind systems are linked at the DC bus and feed power to the grid & the NLLs via a two-level VSC. The system behaviour is assessed under dynamic windspeed, insolation and load unbalancing conditions. Moreover, the cost and efficiency of the hybrid PSC PV-WECS is investigated & compared with that of the conventional PV-wind system.

TABLE 2. Parameters of PSC PV array.

	I_{sc}	V_{oc}	I_{mp}	V_{mp}	P_{max}	Area
Cell	23.5 mA	1.085 V	20.48 mA	0.88 V	0.018 W	0.0001 m^2
Module	4.3 mA	39 V	3.5 mA	30.7 V	0.11 W	0.0018 m^2
Array	67.3 A	751 V	54.48 A	590 V	32.5 kW	82.2 m^2

TABLE 3. Parameters of SPV array.

	I_{sc}	V_{oc}	I_{mp}	V_{mp}	P_{max}	Area
Module	10.44 A	59.12 V	10.29 A	48.6 V	0.5 kW	2.56 m^2
Array	62.64 A	650 V	61.7 A	534 V	32.95 kW	163.8 m^2

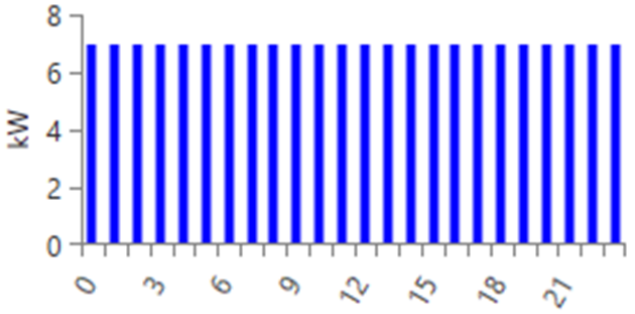

FIGURE 4. The profile of load demand per day.

SA is performed on this system to assess the impact of changing dynamics in the model inputs. This is performed by running numerous optimizations in HOMER under a particular set of input presumptions to evaluate the system performance under varied inputs in terms of NPC & RF.

The proposed PSC PV array delivers the same amount of power by utilising a much smaller space owing to its high efficiency. It reduces the area from 164 m^2 to 82 m^2 which is a whopping decrease of close to 50%. This is detailed in Tables 2 & 3. Moreover, the cost of power production in PSCs is much less as compared to silicon-based devices. It is estimated that the cost of generating 1 watt of power in PSCs varies between 10–20 cents. On the contrary, the cost of generating the same amount of power in silicon-based cells is 75 cents, which is more than four times [23]. The daily load profile of the system is depicted in Fig. 4 with a constant load demand and energy of 7 kW & 168 kWh per day, respectively. A schematic design of the grid-tied RES is shown in Fig. 5. The cost of the components and description of the hybrid system used in this study [31], [32] are given in Table 1. The lifespan of the project is chosen to be 20 years at an interest rate of 8% and zero-capacity shortage. The methodology involving major steps in the techno-economic & SA is illustrated as a flow-diagram in Fig. 6. The outcomes from this study depict an improvement in the cost & efficiency of the proposed PSC PV-WECS system over the conventional SPV-wind system.

A. DYNAMIC PERFORMANCE WITH NLL UNDER LOAD UNBALANCING CONDITIONS

Fig. 7 portrays the response of a grid connected PSC PV-WECS evaluated on the application of a NLL under

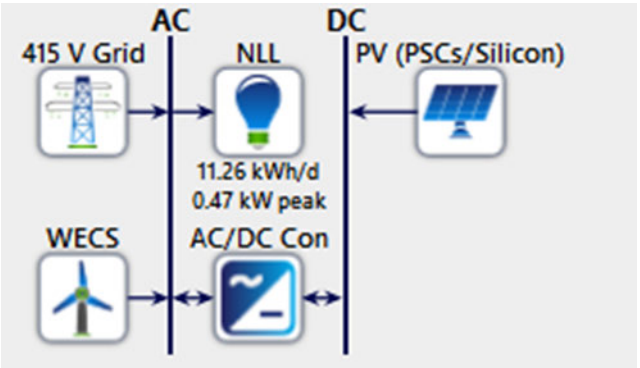

FIGURE 5. The proposed grid-connected PSC-WT hybrid system.

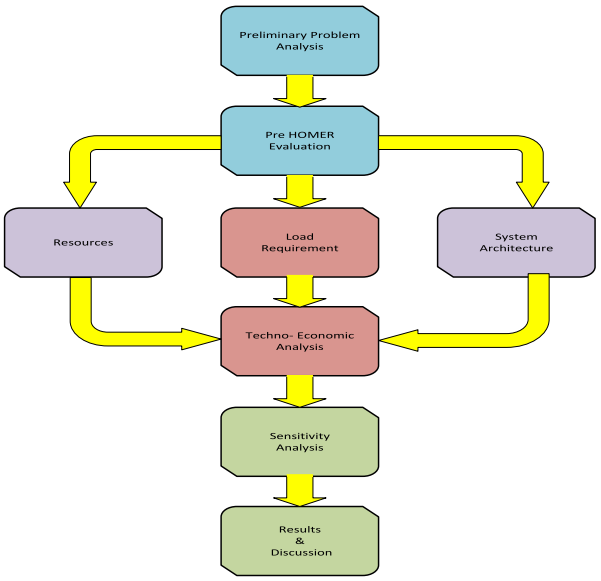

FIGURE 6. Methodology for the economic analysis of the hybrid system.

severe load disturbances. It depicts source side voltage v_{abc}, source side current i_{abc}, load side current i_{Labc}, converter side current i_{vsc}, DC link voltage v_{DC}, wind-voltage v_{wind}, wind-current i_{wind}, wind-power p_{wind}, PSC PV voltage V_{PV}, PSC PV current I_{PV}, PSC PV power p_{PV}, hybrid power P_{total}, irradiance G, wind-velocity v_s, load power p_{load} & grid power p_{grid}. It is evident that net power generated from this hybrid system is 35.6 kW with a demand of 3.78 kW from the load side. The excess power is directed to the grid. At time t = 0.6s, one phase of the load is re-connected with the system swelling the load requirement to 5.58 kW. The DC link voltage is maintained steady at 700 V with no change in the grid current which remains steady and sinusoidal during load unbalancing. Also, hybrid power remains constant and the grid power increases consequently.

B. DYNAMIC PERFORMANCE UNDER CHANGING WIND VELOCITY

The results of the PSC PV-WECS evaluated under changing wind velocity is presented in Figure 8. The total power (7.85 kW) exceeds load power (3.3 kW) and the excess power

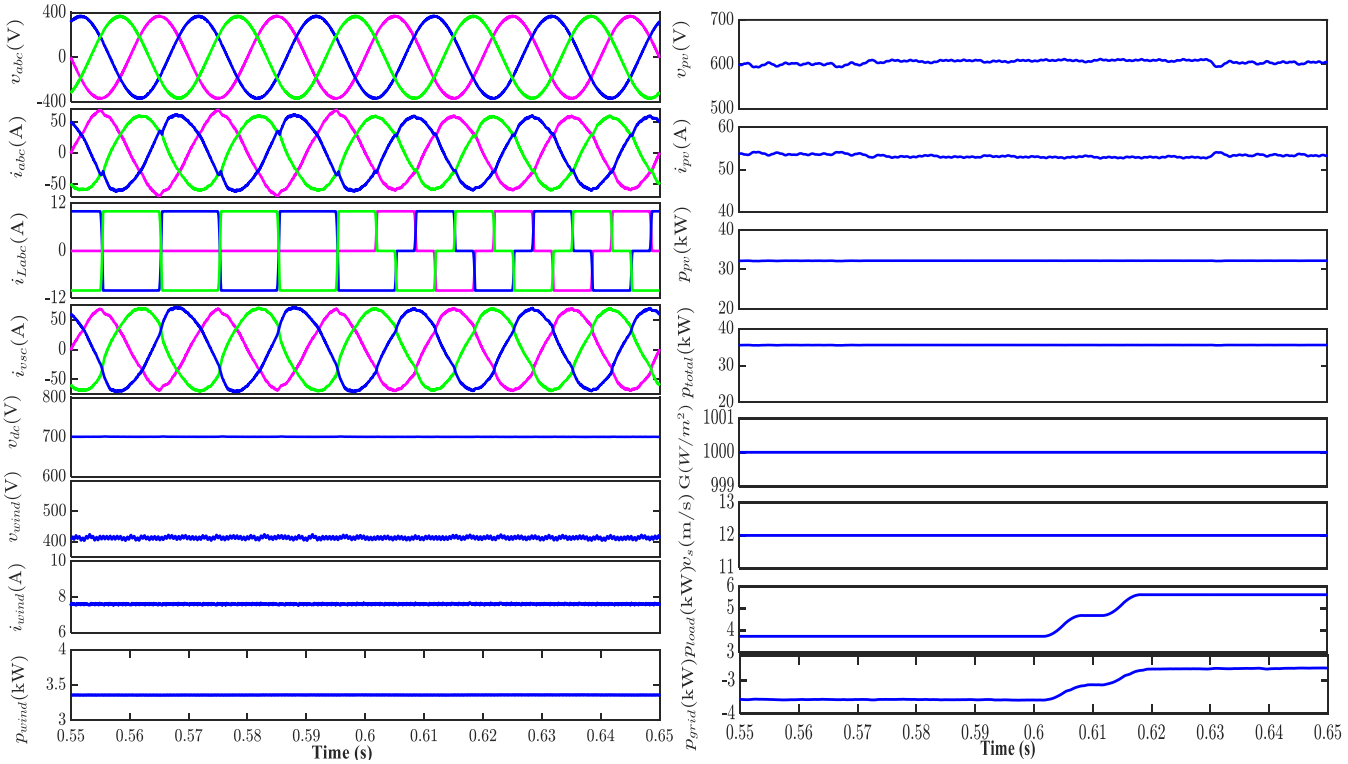

FIGURE 7. Dynamic performance of the PSC PV-WECS under load unbalancing conditions.

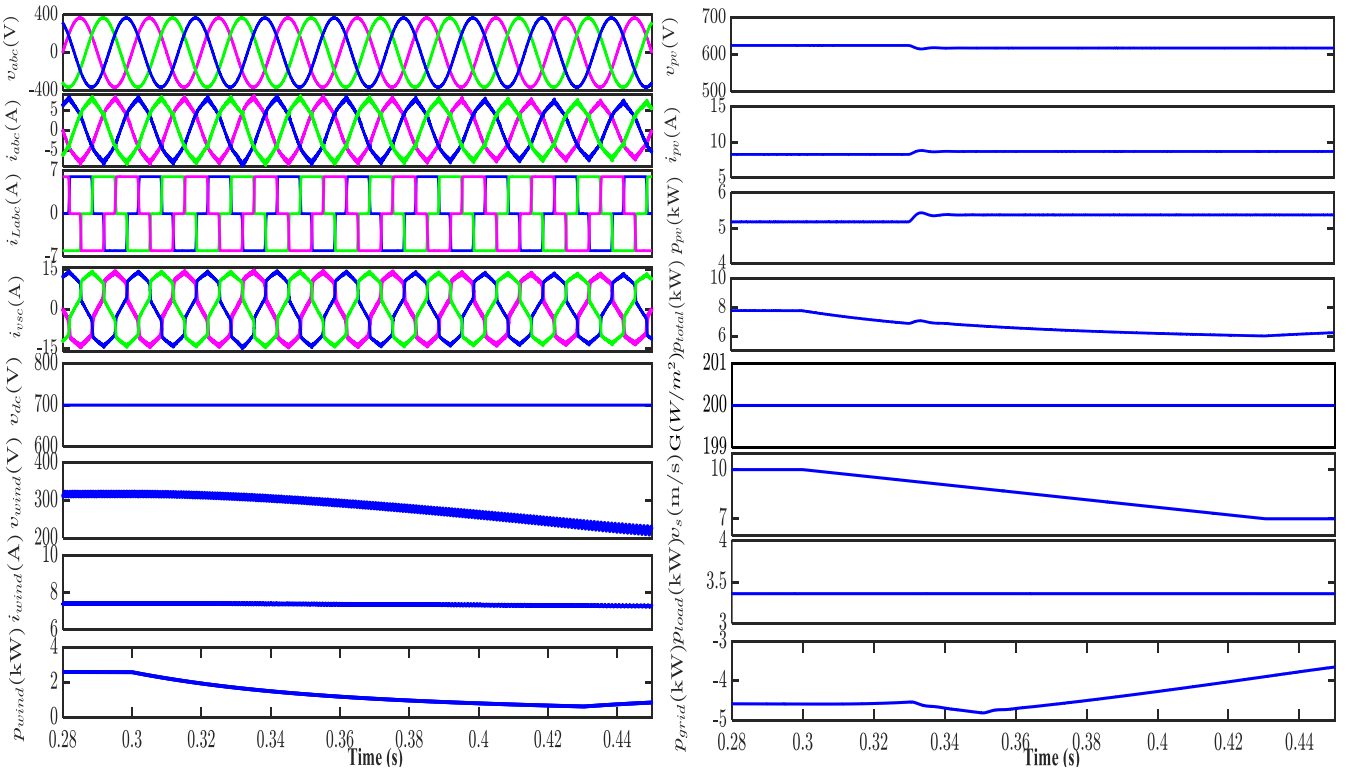

FIGURE 8. Dynamic performance of the PSC PV-WECS under varying windspeed.

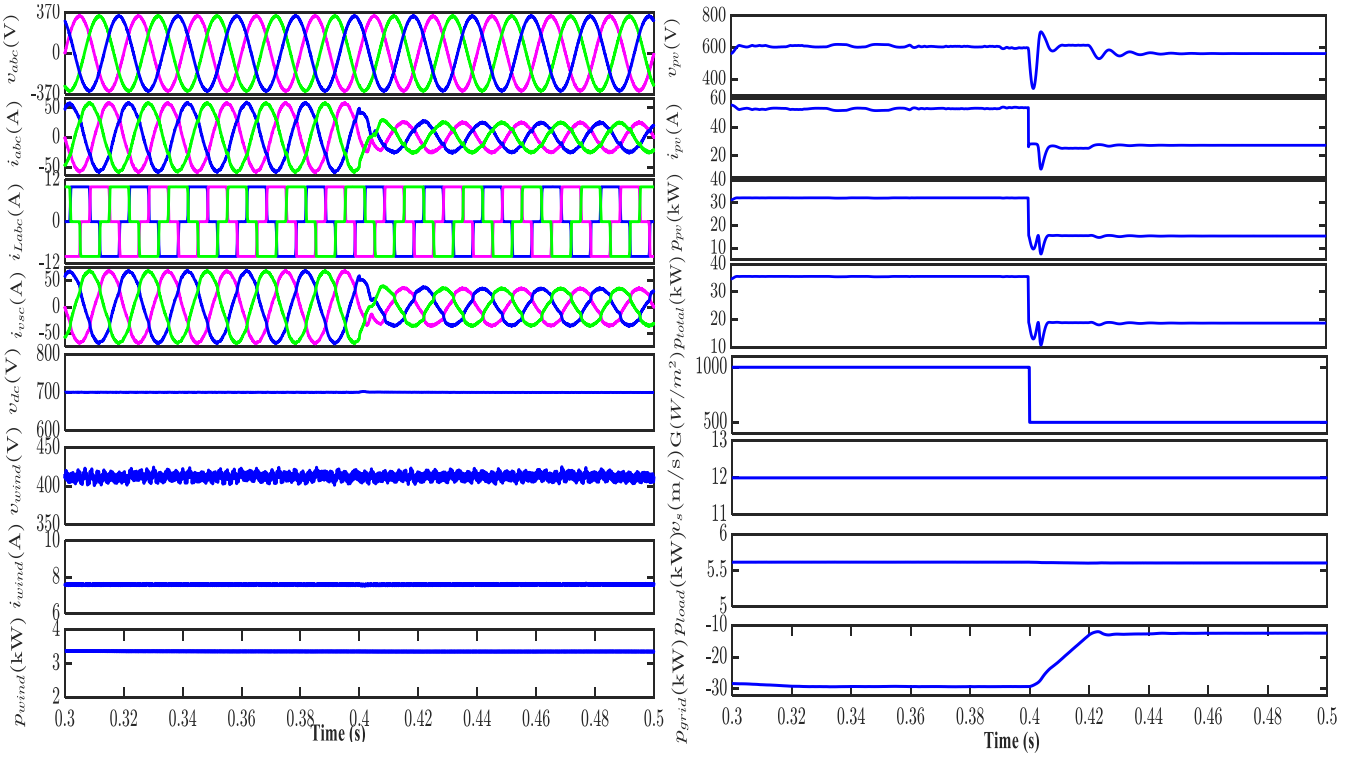

FIGURE 9. Dynamic performance of the PSC PV-WECS under varying insolation.

of 4.55 kW is directed to the grid. At time t = 0.3s, the velocity of wind reduces from 10 m/s to 7 m/s which leads to a decrease in p_{total} and it falls down to 6 kW with no change in p_{load}. As a result, power flowing to the grid reduces. However, the DC link voltage is maintained steady at 700 V throughout.

C. DYNAMIC PERFORMANCE WITH NLL UNDER VARYING INSOLATION

The performance of the proposed system under changing irradiation is presented in Figure 9. p_{pv} is 32.5 kW at an irradiation of 1000 W/m^2 with total power exceeding the load demand. At time t = 0.4s, p_{total} falls to 19 kW owing to decreasing irradiation from 1000 to 500 W/m^2. The deficient power directed to the grid increases as there is no change in load power. The grid side voltages and currents remain sinusoidal and balanced. The DC link voltage remains steady throughout.

D. PROFILE OF WEIGHT SIGNALS

Fig. 10 depicts the ascendancy of the proposed control by comparing the profile of the weight signals with the ones generated in conventional controls. The weight signals in the proposed control converge quickly as compared to the conventional controls where the weights keep oscillating with a large variance about the optimal value. This is because the controlling variable reduces the oscillations from the updated weight and maintains steady weight parameters. The proposed control has lowest oscillations, highest accuracy, and lowest settling time during transient conditions which reduces i_{loss} component and THD.

E. RELATIVE COMPARISON IN TERMS OF NPC AND RF

The relative comparison between PSC PV-WECS & SPV-WECS systems is carried out for the same load & power in Figs. 11 - 16. Table 4 depicts the annual production output of PSC PVs and WT. The PSC PVs generate 89170 kWh/year which is about 82.9% of the total energy output while as the WECS shares 18402 kWh/year which is 17.1% of the total energy produced throughout the year. The comparison of the two systems (PSCs/Wind and PV/Wind) is considered to check the cost of energy of the system with the same conditions. Table 5 depicts the comparison study of the NPC and RFs for PSC PV-WECS & the SPV-WECS. The PSC PV-WECS has a low NPC of $68843 compared to the SPV-WECS whose NPC stands at $160917. This shows that the PSC PV-WECS has reduced the total cost by 58%. This reduction in the NPC in the case of PSC PV-WECS is due to the use of state of the art technologies employed in the manufacture of the PSCs. The RF remains constant at 100% as the grid tied system withdraws power from the RES all the time.

F. SENSITIVITY ANALYSIS

SA aims to ascertain the effects of uncertainties in the system performance on account of varying irradiation and wind speeds for the proposed system. The sensitivity

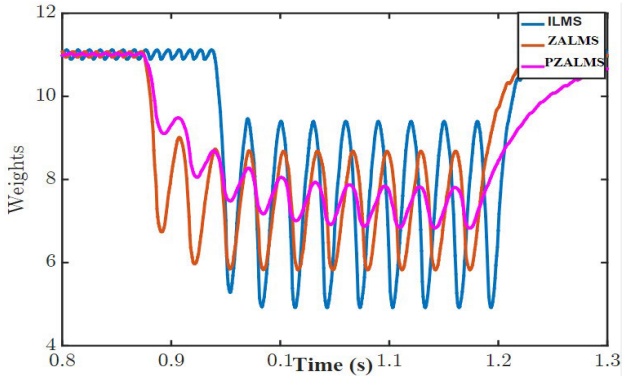

FIGURE 10. Comparison of weights during load unbalancing in different control algorithms.

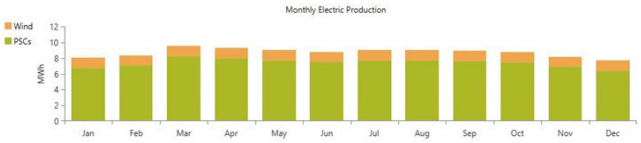

FIGURE 11. Monthly electrical production of PSCs/Wind.

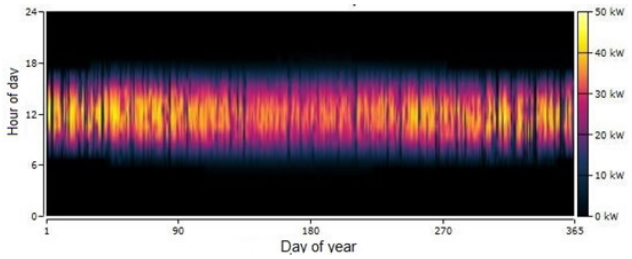

FIGURE 12. THE PSC PV power output sharing throughout the year.

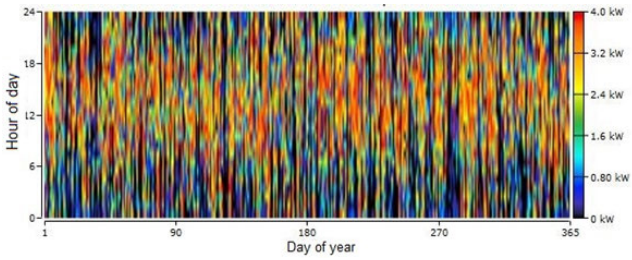

FIGURE 13. THE WT power output sharing throughout the year.

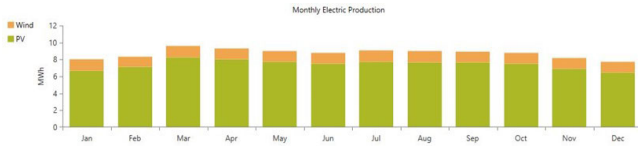

FIGURE 14. Monthly electrical production of SPV/Wind.

variables taken in this study comprise different values of solar irradiance and wind speed to choose the optimum system configuration. In this work, wind speeds were varied from 8 - 12 m/s while as solar insolation was varied from 500 - 1000 W/m^2. The optimized results comprise

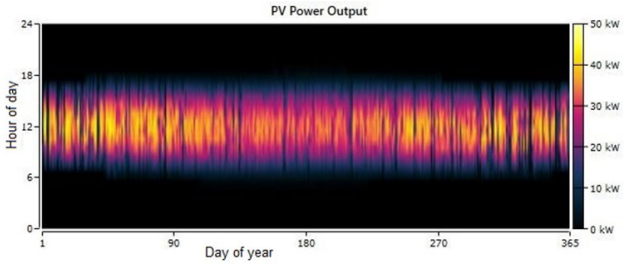

FIGURE 15. THE PV power output sharing throughout the year.

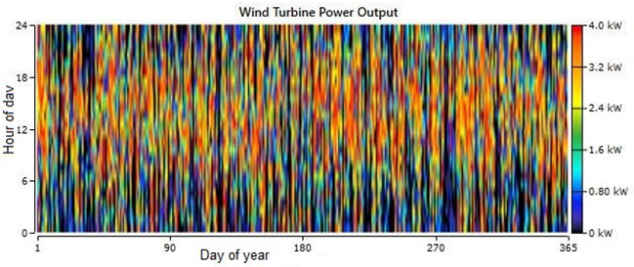

FIGURE 16. THE WT power output sharing throughout the year.

TABLE 4. The yearly production output of PSC PVs and WT.

Production	kW/hour	% Output
LONGI Solar LR6-72PE	89,170	82.9
WT Bergey Excel 10-R	18,402	17.1
Total	107,572	100

TABLE 5. The comparison study of the NPC and RFS for PSC PV-WECS and SPV-WECS.

Technology	NPC ($)	RF (%)
PSC PV-WECS	68843	100
SPV-WECS	160917	100

parameters like the capital cost of the components, NPC and O&M costs.

1) SA IN TERMS OF VARYING WIND SPEED

The SA of the grid-connected PSC PV-WECS in terms of varying windspeed is presented in Table 6. The results of the optimal model are calculated by varying the wind speeds from 9-12 m/s at a fixed load and solar irradiation of 1000 W/m^2. Figs. 17 and 18 represent the optimal results at varying wind speeds of 9 – 12 m/s for a PSC PV-WECS and SPV-WECS, respectively. The results shown in Table 6 reveal that the NPC in the grid tied SPV-WECS case is reduced from $171928 at 9 m/s to $160917 at windspeeds between 10-12 m/s. However, NPC in the grid tied PV PSC-WECS case is reduced considerably from $79853 at 9 m/s to $68843 at windspeeds between 10-12 m/s. This considerable dip in the NPC indicates the superiority of perovskite fabrication. This considerable decrease in NPC from $160917 to $68843 in PSCs translates to a cost reduction of 57% at windspeeds hovering between 10-12 m/s. At windspeeds of 9 m/s, the NPC decreases from $171928 to $79853 leading to a cost reduction of 53%. Figures 17 and 18 reveal that the O&M in the grid tied SPV-WECS case is reduced at increased

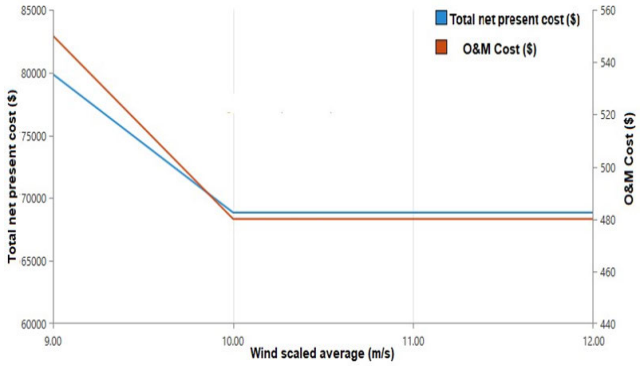

FIGURE 17. Optimal model for PV PSC-WECS at varying wind speed (9 – 12 m/s) and fixed load irradiation.

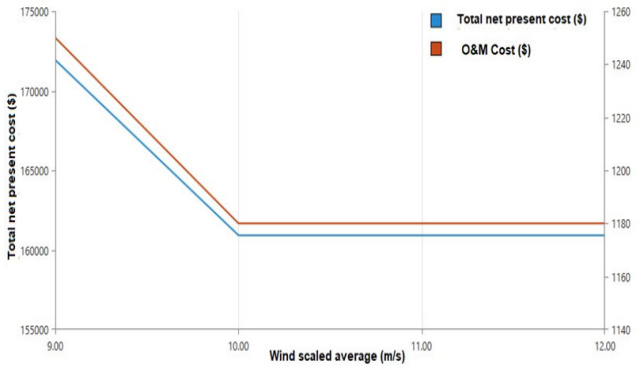

FIGURE 18. Optimal model for SPV-WECS at varying wind speed (9 – 12 m/s) and fixed load irradiation.

TABLE 6. Wind speed sensitivity analysis.

SSC		PSC		
Wind Speed (m/s)	NPC ($)	RF (%)	NPC ($)	RF (%)
12	160917	100	68843	100
11	160917	100	68843	100
10	160917	100	68843	100
09	171928	100	79853	100

windspeeds from $1250 to $1180. However, the O&M is reduced considerably from $550 to $480 with an increase in windspeed from 9 m/s to 11 m/s. The steeper decline in O&M establishes the supremacy of the proposed system. The O&M decrease leads to a cost reduction of 6% for windspeeds hovering between 10-12 m/s and a reduction of 14.6% for a windspeed of 9 m/s.

2) SA IN TERMS OF VARYING INSOLATION

The SA of the grid-connected PSC PV-WECS in terms of varying insolation is compared with that of SPV-WECS at irradiation levels of 500, 600, 700, 800, 900, and 1000 W/m^2. The results of the optimal model for varying solar irradiance (500-1000 W/m^2) at fixed load and wind speed of 12 m/s in PV PSC-WECS and SPV-WECS are presented in Figs. 19 and 20, respectively. Figures 19 and 20 reveal that the NPC (at 500-1000 kWh/m^2 per day) in the grid tied PSC

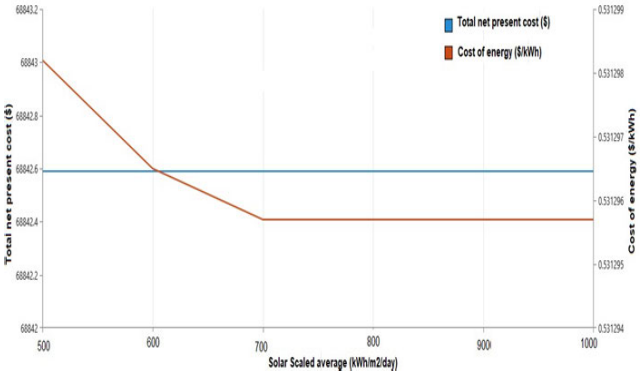

FIGURE 19. Optimal model for PV PSC-WECS at varying insolation (500 – 1000 W/m^2) and fixed wind speed.

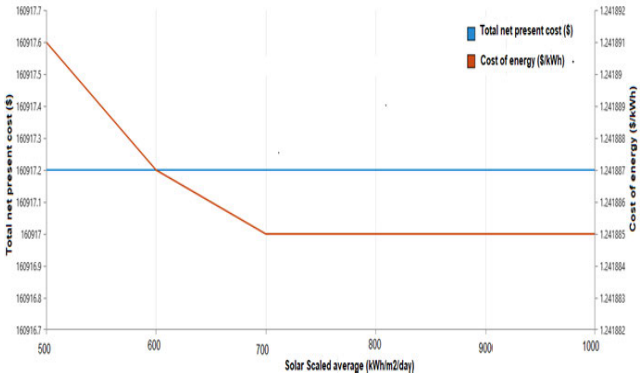

FIGURE 20. Optimal model for SPV-WECS at varying insolation (500 – 1000 W/m^2) and fixed wind speed.

PV-WECS case is $68842.6 as compared to $160917.2 for the SPV-WECS case. This decrease in NPC from $160917.2 in PV SSC to $68842.6 in PV PSC translates to a cost reduction of 52.5% at an irradiation of 500-1000 kWh/m^2 per day. Figures 19 and 20 also reveal that the COE in the grid tied SPV-WECS case reduces in steps with increasing irradiation from $1.24189 /kWh at 500 kWh/$m^2$ per day to $1.241885 /kWh at (700-1000) kWh/m^2 per day. However, the COE in PSC PV-WECS is reduced considerably to $0.5312984/kWh at 500 kWh/m^2 per day and ultimately reduces to 0.5312955/kWh at an irradiation of 700-1000 kWh/m^2 per day. The reduced COE establishes the supremacy of the proposed system.

VI. CONCLUSION

This paper presents the design of a three-phase grid-connected PSC PV-WECS capable to deal with varying scenarios like changing wind velocity and insolation and unbalanced NLL. Power flows from the system to the grid & the NLLs through a VSC which is controlled by PZALMS algorithm. The proposed control extracts accurate loss component of current & generates precise gating pulses which enhances the performance of the system in terms of reduced DC bus transients during dynamic conditions. It also removes grid harmonics which enhances PQ of

the system. Moreover, the economic analysis between PSC PV-WECS and SPV-WECS is carried out in this work. The PSC PV-WECS has a low NPC of $68843 compared to $160917 in case of SPV-WECS. This reduces the total cost in PSC PV-WECS by 58%. This reduction in the NPC is due to the use of new technologies in the manufacture of the PSCs which improves their efficiency. The effect of varying irradiation & windspeed is studied by varying the insolation from 500-1000 W/m^2 per day in steps of 100. The results of the optimal model of PV PSC-WECS for varying solar insolation (500-1000 kWh/m^2 per day) at fixed load and wind speed of 12 m/s is considered. The COE decreased by 57% from $160917 in SPV-WECS to $68843 in PSC PV-WECS systems. The results of the optimal model of PSC PV-WECS for varying wind speed (9 – 12 m/s) at fixed load and solar irradiation of 1000 W/m^2 per day is considered.

The results of SA depict the dependence of optimal solutions on the uncertainty of key variables for a fixed system configuration presented in this work. SA with four varying variables namely NPC, COE, windspeed & insolation demonstrate the sensitivity of the total NPC with regard to each variable. The results show that the total NPC is more sensitive to the COE and the average wind speed as compared to the other variables. Moreover, the NPC of PSC PV-WECS is much lower as compared to SPV-WECS giving way to high efficiency & increased economic benefits. Such information can come handy for a designer in reducing the effects of uncertain variables in a grid connected hybrid system and can be used as a guideline on the design and implementation of grid-connected wind and PV-systems.

REFERENCES

[1] A. A. Zaky, E. Christopoulos, K. Gkini, M. K. Arfanis, L. Sygellou, A. Kaltzoglou, A. Stergiou, N. Tagmatarchis, N. Balis, and P. Falaras, "Enhancing efficiency and decreasing photocatalytic degradation of perovskite solar cells using a hydrophobic copper-modified titania electron transport layer," *Appl. Catal. B, Environ.*, vol. 284, May 2021, Art. no. 119714.

[2] *Solar Cells Efficiency Map*. Accessed: Nov 5, 2022. [Online]. Available: https://www.nrel.gov/pv/cell-efficiency.html

[3] S. Wang, P. Wang, B. Chen, R. Li, N. Ren, Y. Li, B. Shi, Q. Huang, Y. Zhao, M. Grätzel, and X. Zhang, "Suppressed recombination for monolithic inorganic perovskite/silicon tandem solar cells with an approximate efficiency of 23%," *eScience*, vol. 2, no. 3, pp. 339–346, May 2022. [Online]. Available: https://www.sciencedirect.com/science/article/pii/S2667141722000404

[4] A. A. Zaky, M. N. Ibrahim, I. B. M. Taha, B. Yousif, P. Sergeant, E. Hristoforou, and P. Falaras, "Perovskite solar cells and thermoelectric generator hybrid array feeding a synchronous reluctance motor for an efficient water pumping system," *Mathematics*, vol. 10, no. 14, p. 2417, Jul. 2022.

[5] H. Rezk, M. M. Elsenety, S. Ferahtia, P. Falaras, and A. A. Zaky, "A novel parameter identification strategy based on COOT optimizer applied to a three-diode model of triple cation perovskite solar cells," *Neural Comput. Appl.*, vol. 35, no. 14, pp. 10197–10219, May 2023.

[6] A. Olabi, H. Rezk, M. Abdelkareem, T. Awotwe, H. Maghrabie, F. Selim, S. Rahman, S. Shah, and A. Zaky, "Optimal parameter identification of perovskite solar cells using modified bald eagle search optimization algorithm," *Energies*, vol. 16, no. 1, p. 471, Jan. 2023.

[7] J. Xu, C. C. Boyd, Z. J. Yu, A. F. Palmstrom, D. J. Witter, B. W. Larson, R. M. France, J. Werner, S. P. Harvey, and E. J. Wolf, "Triple-halide wide–band gap perovskites with suppressed phase segregation for efficient tandems," *Science*, vol. 367, no. 6482, pp. 1097–1104, 2020.

[8] O. Ayan and B. E. Turkay, "Techno-economic comparative analysis of grid-connected and islanded hybrid renewable energy systems in 7 climate regions, Turkey," *IEEE Access*, vol. 11, pp. 48797–48825, 2023.

[9] Y. Ayed, R. Al Afif, P. Fortes, and C. Pfeifer, "Optimal design and techno-economic analysis of hybrid renewable energy systems: A case study of Thala city, Tunisia," *Energy Sour., B, Econ., Planning, Policy*, vol. 19, no. 1, Dec. 2024, Art. no. 2308843.

[10] P. K. Kushwaha and C. Bhattacharjee, "An extensive review of the configurations, modeling, storage technologies, design parameters, sizing methodologies, energy management, system control, and sensitivity analysis aspects of hybrid renewable energy systems," *Electr. Power Compon. Syst.*, vol. 51, no. 20, pp. 2603–2642, Dec. 2023.

[11] R. K. Agarwal, I. Hussain, and B. Singh, "LMF-based control algorithm for single stage three-phase grid integrated solar PV system," *IEEE Trans. Sustain. Energy*, vol. 7, no. 4, pp. 1379–1387, Oct. 2016.

[12] R. K. Agarwal, I. Hussain, and B. Singh, "Application of LMS-based NN structure for power quality enhancement in a distribution network under abnormal conditions," *IEEE Trans. Neural Netw. Learn. Syst.*, vol. 29, no. 5, pp. 1598–1607, May 2018.

[13] N. Kumar, B. Singh, and B. K. Panigrahi, "LLMLF-based control approach and LPO MPPT technique for improving performance of a multifunctional three-phase two-stage grid integrated PV system," *IEEE Trans. Sustain. Energy*, vol. 11, no. 1, pp. 371–380, Jan. 2020.

[14] M. I. Nazir, A. Ahmad, and I. Hussain, "Improved higher order adaptive sliding mode control for increased efficiency of grid connected hybrid systems," *Int. J. Emerg. Electric Power Syst.*, vol. 22, no. 5, pp. 583–594, Oct. 2021.

[15] M. I. Nazir, Y. Irshad, I. Hussain, and A. Ahmad, "Experimental implementation of optimally tuned multifunctional RLMLS driven VSC tied to single phase voltage weak distribution grid," *J. Ambient Intell. Humanized Comput.*, vol. 14, no. 4, pp. 4561–4572, Apr. 2023.

[16] N. Kumar, B. Singh, B. K. Panigrahi, and L. Xu, "Leaky-least-logarithmic-absolute-difference-based control algorithm and learning-based InC MPPT technique for grid-integrated PV system," *IEEE Trans. Ind. Electron.*, vol. 66, no. 11, pp. 9003–9012, Nov. 2019.

[17] M. I. Nazir, A. Ahmad, and I. Hussain, "Filtered X least mean fourth-driven intelligent control for power quality augmentation and dynamic stability reinforcement of grid intertie wind–photovoltaic systems," *Int. J. Circuit Theory Appl.*, vol. 50, no. 12, pp. 4492–4516, Dec. 2022.

[18] M. I. Nazir, A. Ahmad, and I. Hussain, "Water cycle algorithm based parametric tuning of non-negative LMMN control of grid tied renewable energy systems," *IETE J. Res.*, vol. 69, no. 12, pp. 9428–9444, Dec. 2023.

[19] D. D. Martínez, R. T. Codorniu, R. Giral, and L. V. Seisdedos, "Evaluation of particle swarm optimization techniques applied to maximum power point tracking in photovoltaic systems," *Int. J. Circuit Theory Appl.*, vol. 49, no. 7, pp. 1849–1867, Jul. 2021, doi: 10.1002/cta.2978.

[20] A. F. Tazay, A. M. A. Ibrahim, O. Noureldeen, and I. Hamdan, "Modeling, control, and performance evaluation of grid-tied hybrid PV/Wind power generation system: Case study of Gabel El-Zeit region, Egypt," *IEEE Access*, vol. 8, pp. 96528–96542, 2020.

[21] B. S. V. Sai, D. Chatterjee, S. Mekhilef, and A. Wahyudie, "An SSM-PSO based MPPT scheme for wind driven DFIG system," *IEEE Access*, vol. 10, pp. 78306–78319, 2022.

[22] *Perovskite Solar Cells: An In-Depth Guide + Comparisons With Other Techs*. Accessed: May 16, 2022. [Online]. Available: https://solarmagazine.com/solar-panels/perovskite-solar-cells

[23] M. De Bastiani, V. Larini, R. Montecucco, and G. Grancini, "The levelized cost of electricity from perovskite photovoltaics," *Energy Environ. Sci.*, vol. 16, no. 2, pp. 421–429, 2023.

[24] S. M. Dawoud, "Techno-economic and sensitivity analysis of hybrid electric sources on off-shore oil facilities," *Energy*, vol. 227, Jul. 2021, Art. no. 120391.

[25] M. Khalid, "Smart grids and renewable energy systems: Perspectives and grid integration challenges," *Energy Strategy Rev.*, vol. 51, Jan. 2024, Art. no. 101299.

[26] D. Temene Hermann, N. Donatien, T. Konchou Franck Armel, and T. René, "Techno-economic and environmental feasibility study with demand-side management of photovoltaic/wind/hydroelectricity/battery/diesel: A case study in sub-saharan Africa," *Energy Convers. Manage.*, vol. 258, Apr. 2022, Art. no. 115494.

[27] P. Li and H. Zhao, "A polynomial zero attracting affine projection algorithm for sparse system identification," *IFAC-PapersOnLine*, vol. 52, no. 24, pp. 308–311, 2019. [Online]. Available: https://www.sciencedirect.com/science/article/pii/S2405896319323353

[28] Z. Luo, H. Zhao, and X. Zeng, "A class of diffusion zero attracting stochastic gradient algorithms with exponentiated error cost functions," *IEEE Access*, vol. 8, pp. 4885–4894, 2020.
[29] B. Singh, A. Chandra, and K. Al-Haddad, *Power Quality: Problems and Mitigation Techniques*. Hoboken, NJ, USA: Wiley, 2014.
[30] F. Fazelpour, N. Soltani, and M. A. Rosen, "Feasibility of satisfying electrical energy needs with hybrid systems for a medium-size hotel on Kish Island, Iran," *Energy*, vol. 73, pp. 856–865, Aug. 2014.
[31] S. M. Dawoud, F. Selim, X. Lin, and A. A. Zaky, "Techno-economic and sensitivity investigation of a novel perovskite solar cells based high efficient hybrid electric sources for off-shore oil ships," *IEEE Access*, vol. 11, pp. 41635–41643, 2023.
[32] S. M. Dawoud, M. R. Elkadeem, M. A. Abido, E. G. Atiya, X. Lin, A. S. Alzahrani, and K. M. Kotb, "An integrated approach for cost- and emission optimal planning of coastal microgrid with demand-side management," *Sustain. Cities Soc.*, vol. 101, Feb. 2024, Art. no. 105149.

MASOOD IBNI NAZIR (Member, IEEE) received the B.E. degree from the Government College of Engineering and Technology, Jammu, India, in 2013, the M.Tech. degree from Vellore Institute of Technology, Vellore, India, in 2016, and the Ph.D. degree from the National Institute of Technology Srinagar, India, in 2022. He is currently an Assistant Professor with the Department of Electrical Engineering, College of Engineering and Information Technology, Saudi Arabia. His research interests include power quality, adaptive converter controls, and grid-connected renewable energy systems.

F. SELIM has been an Associate Professor with the Department of Electrical Engineering, Kafrelsheikh University, since 2020. His current research interests include renewable energy, solar energy technologies, high-voltage, optimization, and power system operation and control.

AIJAZ AHMAD (Member, IEEE) received the B.E. degree in electrical engineering from the National Institute of Technology (NIT) Srinagar, India, in 1984, and the M.Tech. and Ph.D. degrees from Indian Institute of Technology, New Delhi, India, in 1991 and 1998, respectively. He is currently a Professor with the Department of Electrical Engineering, NIT Srinagar. His research interests include power system operation and optimization, power system restructuring and deregulation, and FACTS.

IKHLAQ HUSSAIN received the B.E. degree in electrical from the University of Jammu, Jammu, India, in 2009, the M.Tech. degree in electrical power system management from Jamia Millia Islamia, New Delhi, India, in 2012, and the Ph.D. degree from the Indian Institute of Technology Delhi, New Delhi, in 2018. He is currently an Assistant Professor with the Department of Electrical Engineering, NIT Srinagar. His research interests include power quality, custom power devices, and renewable energy systems.

SAMIR M. DAWOUD received the B.Sc. and M.Sc. degrees in electrical power and machines engineering from Tanta University, Egypt, and the Ph.D. degree in electrical engineering from Huazhong University of Science and Technology, China, in 2017. He is currently an Associate Professor with the Electrical Engineering Department, Tanta University. His current research interests include renewable energy, power system planning, microgrid planning optimization, and power system reliability.

KHALIL ALLUHAYBI (Member, IEEE) received the B.S. degree in electrical engineering from Taibah University, Medina, Saudi Arabia, in 2012, and the M.S. and Ph.D. degrees in electrical engineering from the University of Central Florida, Orlando, FL, USA, in 2017 and 2020, respectively. He is currently an Assistant Professor with the Electrical Engineering Department, Taibah University. He is also a Senior Research Fellow with Florida Power Electronic Center (FPEC), University of Central Florida, and an Associate Researcher with the Power Conversion and Power Management Center, Nanjing, China. His current research interests include inverter topologies for photovoltaic (PV) applications, digital control in power electronics, efficiency optimization of dc/ac inverters, and soft switching techniques.

ALAA A. ZAKY received the B.Sc. degree in electrical power and machines engineering from Kafrelsheikh University, Egypt, in 2007, the M.Sc. degree in electrical power and machines engineering from Mansoura University, Egypt, in 2015, and the Ph.D. degree in electrical engineering from the School of Electrical and Computer Engineering, National Technical University of Athens, in 2021. He has been an Assistant Professor with the Department of Electrical Engineering, Kafrelsheikh University, since 2021. His current research interests include renewable energy, solar energy technologies, third-generation solar cells, optimization, and power system operation and control.